www.elsevier.nl/locate/jorganchem

Journal of Organometallic Chemistry 617–618 (2001) 647–655

Journal of Organometallic Chemistry

Evidence for multiple bonding in four-coordinate, cationic, platinum–thiosilylenes via AIM and CDA; effects of phosphine choice

Frederick P. Arnold, Jr.

Department of Chemistry/Academic Technologies, Northwestern University, 2145 Sheridan Road, Evanston, IL 60208, USA

Received 5 September 2000; accepted 4 October 2000

Abstract

Hybrid DFT/HF calculations were performed on five complexes $(PH_3)_2(H)Pt–Si(SH)_2^+$, $(PH_3)_2(H)Pt–Si(SMe)_2^+$, $(PMe_3)_2(H)Pt–Si(SMe)_2^+$, $(P^iPr_3)_2(H)Pt–Si(SEt)_2^+$, and $(PCy_3)_2(H)Pt–Si(SEt)_2^+$, and analyzed using CDA and Atoms-In-Molecules. Complexes were found to possess both Si–S and Si–Pt multiple bond character, in contrast to earlier results at lower levels of theory. The origins of twisted geometries were determined to be primarily steric in nature. Increasing the size of aliphatic substituents on the phosphines leads to a more balanced bonding motif, but increases steric repulsion, while changing the substituent at silicon from hydrogen to methyl resulted in a lengthening of the Si–Pt bond. Based on these results, the use of PH_3 to substitute for PMe_3 and larger groups in calculations is discouraged, though methyl is an acceptable, if not electronically identical, substitute for larger aliphatic phosphines. © 2001 Published by Elsevier Science B.V.

1. Introduction

The synthesis of planar silylenes possessing metal–silicon double bonds has been an interesting but difficult problem for many years [1]. The formation of double bonds between silicon and a transition metal is hampered by a number of factors, including diffuse valence orbitals [2] and the electropositive nature of the silicon. Consequently, most of the observed metal–silylene complexes possess some stabilization of the silicon center through donation from a Lewis base [3]. This stabilization may take one of three forms; intermolecular, where a strong base, such as HMPA or THF associates through an available lone-pair on the solvent with the vacant p-orbital on silicon, leading to pyramidalization of the Si center and bond-lengthening (Fig. 1(A)); intramolecular-σ, where a basic functionality on a ligand coordinates to the vacant orbital (Fig. 1(B)) [4], and intramolecular-π, where an atom possessing a lone-pair, directly bonded to the silicon center, is capable of forming a π-bond through a donor–acceptor arrangement (Fig. 1(C)). Until the mid 1990s, when Tilley and coworkers, among others, synthesized a number of complexes possessing the intra-molecular-π coordination [5], most of the known examples were solvent-stabilized. Ziegler provided a solid theoretical justification for the preference for binding a solvent molecule versus stabilizing a multiple bond [6], which indicated that these systems should exist as discrete silylenes in the absence of solvent, but were significantly stabilized by the addition of σ-bound solvent molecules. For the third type, early theoretical work-ups of these systems using Fenske–Hall [7], indicated that the observed bonding was primarily a π-bond between the main-group atoms, with little or no π-interaction between Si and the metal [5c,8]; however, more recent work indicated that in the case of the ruthenium–thiosilylene complexes that some multiple bonding may exist [9].

Despite the evidence against the existence of a metal to silicon multiple-bond in the intramolecular-base-stabilized complexes, tantalizing evidence to the contrary exists; the systems are shown by NMR to possess hindered rotation about the Si–Pt bond. The metal to silicon bonds were shorter than those observed for either $M–SiR_3$ type bonds, or the intermolecular donor-

E-mail address: f-arnold@northwestern.edu (F.P. Arnold, Jr.).

0022-328X/01/$ - see front matter © 2001 Published by Elsevier Science B.V.
PII: S0022-328X(00)00737-3

stabilized systems, and the coordination about the silylene fragment was strongly planar. Since the earlier work was performed on the class of cationic, 4-coordinate complexes, shown schematically in Fig. 2, it was decided to return to these complexes to investigate the problem of multiple bonding in metal to silylene complexes possessing the capability of intramolecular π-bonding.

2. Computational

All calculations were performed using Gaussian 98 rev A7 [10]. Complexes were optimized using the B3LYP hybrid functional and the LANL2DZ effective core potentials and associated valence basis set for Pt and all atoms directly connected to Pt. This ECP/basis set combination uses the D95 all electron basis set for H–Ne, and ECPs on Pt, Si, P, and S. The LANL2DZ basis set was further augmented by d-functions on the Si, S, and P atoms and p-functions on the hydrogen. The carbons attached to the carbons used the LANL2DZ basis set, without augmentation. This is referred to as basis set **I** [11]. For the complexes $(PR_3)_2(H)Pt–Si(SY)_2^+$, (R = Me, H, ^{i}Pr, Y = H, Me) minima were confirmed by vibrational analysis. For (R = Cy, Y = Et), this complex was too large to complete such an analysis, and so instead small perturbations to the structure were made, and the structure allowed to relax to the minima. Variations of less than 0.0001 Hartree total energy and displacements of less than 0.005 Å, all confined to the movements of hydrogens, led to the conclusion that it was also close enough to the global minimum to be considered optimized for the purposes of this study. Charge density analysis was carried out using CDA 2.1 [12], with the systems partitioned into the fragments $(PR_3)_2(H)Pt^+$ and $Si(SY)_2$ to describe the Pt–Si bonding, and into the fragments $(PR_3)_2$ and $(H)Pt–Si(SY)_2^+$ to describe the phosphine to metal bonding [13]. The CDA analysis employed basis set I, at the optimized geometries [14]. Bond energies from the CDA method are simply the energy of the complex minus the energies of the fragments. They are therefore not the same as the true bond energy, which would allow the fragments to relax to their isolated lowest energy structure. Single point calculations at the minimum geometries were performed using the Huzinaga (432222/4222/423/3) basis set for platinum [15], with the outermost s, p, and d functions uncontracted, and augmented by two p-type polarization functions [16], yielding a (4322211/42211 + + /42111/3) contraction, and the 6-311 + + G for the main-group elements in order to obtain wavefunction files for AIM analysis (basis set **II**). AIM analysis was performed using EXTREME (ext94b) to locate and characterize the critical points, and PROAIMV 94b [17] to calculate the charges. AIM2000 from Biegler-König's group was used to trace the bond-paths [18]. Charges were calculated using the PROAIM algorithm for the R = H, Me systems, and PROMEGA for R = ^{i}Pr, due to the complex topology of the electron density of the system. Charges and properties were not determined for the complex R = Cy due to size and problems caused by the complex topology of the electron density. See the text for further details.

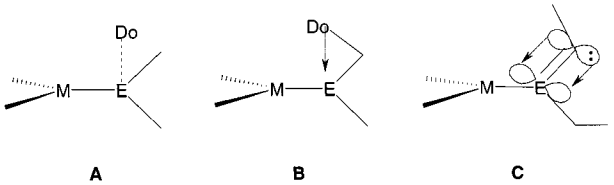

Fig. 1. Schematic diagram of modes of base-stabilization in metal to main-group complexes: (A) intermolecular, (B) intramolecular σ, (C) intramolecular π.

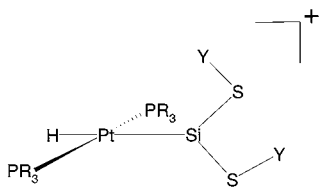

Fig. 2. Geometry of a cationic, planar, four-coordinate, metal silylene. In the limiting case, the S–Si–S plane is perpendicular to the P–Pt–P plane. Distortions from this geometry are steric in nature.

Effects of correlation on the Si–Pt bond distance were determined using Basis set I on the minimal complex with R = H, Y = H, and the functionals BLYP and B3LYP, as well as the more traditional MP2 method. The bond distance increases steadily from 2.338 Å (MP2) to 2.368 Å (B3LYP) to 2.384 Å (BLYP), a total increase of 0.046 Å, or approximately 2%. The Pt–Si distance from the MP2 calculation is still 0.068 Å longer than the experimentally determined distance of 2.270 Å, indicating that the observed discrepancy between the model complex and the experimentally characterized complex is due to the nature of the ligands, and not the level of theory employed.

3. Results and discussion

In Table 1 are seen selected geometrical parameters of the five complexes. The model with R = H has the longest bond distance, which shortens as hydrogen is replaced by methyl on the phosphine. Substituting methylthiol (MeS) for thiol (HS) results in a slight bond lengthening (Pt–Si) of 0.02 Å, and a shortening of the Si–S bond, by approximately the same amount. This indicates that the observed Pt–Si bond distance, and hence degree of π-character, is largely determined by

Table 1
Selected geometrical parameters for $(PR_3)_2(H)Pt–Si(SY)_2^+$

R	Y	*r*PtSi	*r*PtP	*r*SiS	Dihedral
H	H	2.368	2.337	2.103	0.0
H	Me	2.380	2.331	2.092	0.0
Me	Me	2.319	2.373	2.101	0.0
^{i}Pr	Et	2.309	2.403	2.108	7.6
Cy	Et	2.306	2.401	2.112	9.1
Cy*	Et*	2.270	2.298	2.081	13.9

Table 3
AIM charges for Pt, Si, S, P, and H (bonded to Pt)

R	Y	Pt	Si	S	P	H(Pt)
H	H	−0.001	1.456	−0.557	1.819	−0.145
H	Me	−0.001	1.452	−0.628	1.816	−0.155
Me	Me	−0.007	1.453	−0.646	1.718	−0.206
^{i}Pr	Et	−0.099	1.469	−0.677	1.218	−0.183
Cy	Et	–	–	–	–	–

the nature of the phosphine rather than by the substituents at silicon. This subtle interplay between the charges and electron densities of the various atoms, (which may be seen in Tables 2 and 3), nicely balances the *trans*-effect as the ligand set at platinum is varied. In the small models, there does not exist sufficient electron donating ability on the phosphine, and hence on the metal, to overcome the effect of a hydridic hydrogen *trans* to a weakly electronegative element such as silicon. As the σ-donor nature of the phosphine is strengthened, the platinum gains electron density, which strengthens the Pt–Si back-bond, thereby weakening the relative magnitude of the hydrogen's influence, and causing the Pt–Si bond to contract. For the model complex with the same ligands as the experimentally determined parent molecule it is seen that the Si–Pt bond distance is very close (2.306 vs. 2.270 Å, 0.036 Å difference) to the experimental value, and the Pt–P distance is long by approximately 0.1 Å. The calculated bond lengths of the highly substituted complexes are in good agreement with the experimentally determined structures, with the discrepancies in bond-length consistent with that expected due to lack of explicit inclusion of relativistic effects [19].

The geometries are also noteworthy in that the experimentally observed twisting of the silylene group with respect to the metal–phosphine fragment seems to be sterically derived [20]. When the substituents are relatively small, such as in the (R = Me, Y = Me) case, the complex prefers to adopt a structure of approximately Cs symmetry, with no twist between the two planes. On the other hand, as steric bulk is added, (Fig. 3, R = Cy, Y = Et), the possible stable configurations become fewer in nature, and an approximately 10° twist is observed. This configuration is the result of the rotation of the cyclohexyl groups with respect to each other and to the ethyl groups in order to minimize the steric interactions. The final configuration, which mimics well the crystal structure, shows a groove in which the ethyl group sits, minimizing interactions between it and the phosphines, and slightly twisted from perpendicular.

Tables 2 and 3 summarize the AIM calculations, presenting the character of the (3,-1) Si–Pt critical point, the Si–S critical points, and the atomic charges. The silicon is highly charged in all of the complexes, but the phosphorus atoms possess a greater charge, as a result of not being associated with a strong Lewis base. The hydrogen atoms directly attached to the P or S groups have a charge of approximately −0.5, while the hydrogen attached to the platinum possesses a charge of −0.15 to −0.20. The integrated charge of the hydrogens attached to the aliphatic ligands on the phosphine are approximately 0.05, which is essentially neutral, and contrasts with the charge of −0.51 when directly connected to the phosphorous in PH_3. As the substituents on P and S increase in size, the charges of the heavy atoms become less positive. This causes a shift in the charge of the phosphine ligand to go from approximately +0.5 in PH_3 to 0.0 in PMe_3, which means that if unperturbed by the SiY_2^+ group, the Pt exists in a d^0 state. The charges of the two fragments, the platinum and silylene, are over all a fairly consistent +0.5, +0.5. While surprising at first, this is a byproduct of the high positive charge of the phosphorus centers, and the strong negative charge of the thiols.

Table 2
(3,-1) selected properties of the Pt–Si and Si–S bond critical points [a]

R	Y	Pt–Si				Si–S			
		ρ	ε	$\nabla^2\rho$	$H(r)$	ρ	ε	$\nabla^2\rho$	$H(r)$
H	H	0.086	0.149	0.078	−0.0323	0.105	0.159	0.159	−0.0675
H	Me	0.084	0.143	0.072	−0.0315	0.106	0.176	0.176	−0.0680
Me	Me	0.092	0.146	0.060	−0.0391	0.105	0.168	0.168	−0.0665
^{i}Pr	Et	0.092	0.151	0.056	−0.0404	0.104	0.150	0.150	−0.0656
Cy	Et	–	–	–	–	–	–	–	–

[a] Units are: ρ (e/a_0^3), $\nabla^2\rho$ (e/a_0^5), $H(r)$ (Hartree/a_0^3).

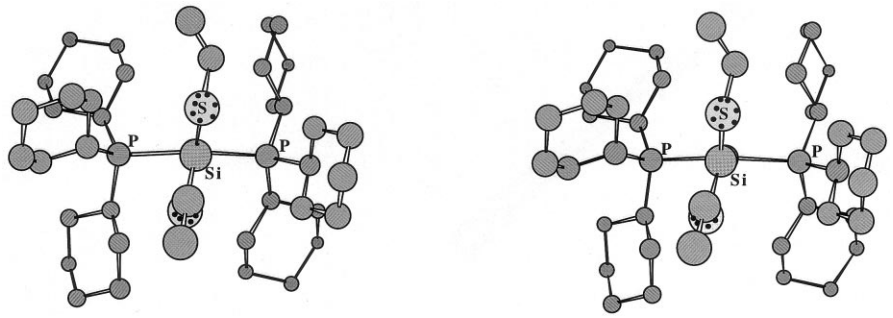

Fig. 3. Relaxed eye stereoplot of $(PCy_3)_2(H)PtSi(SEt)_2^+$, looking down the Si–Pt axis. Note how the steric interactions of the cyclohexyl groups creates a narrow, and off-perpendicular channel, into which the ethyl groups may nestle. This off-axis twist disappears with decreasing steric bulk. Key: silicon, phosphorus, sulfur: as labeled, C: grey circles. Pt is obscured by Si in this view, hydrogens have been omitted for clarity.

So, while the charges of the individual atoms may be high, the charge of the fragments are such that overall the positive charge on the system is distributed fairly evenly over the two fragments, but localized on the silicon and phosphorus atoms. This is somewhat visible in Fig. 6, where it may be seen that the atomic basins around Si and P show little charge accumulation, with most of it being polarized towards the atoms which they are bonded to. The sudden reduction in charge at phosphorus upon changing from PMe_3 to P^iPr_3 may be explained by the replacements of two of the methyl hydrogens with methyl groups. This causes a decrease in charge at the carbon bonded to the phosphorus from -0.58 when it's a methyl carbon, to -0.40, when it's the central carbon of an isopropyl. This would lead one to conclude that to appropriately model the electronic or charge effects of larger phosphines, that the 1-4 connectivity of the phosphine substituent (M–P–R–R′, Fig. 4) is more important than the specific phosphine, i.e. while trimethylphosphine is probably a good substitute for triethylphosphine or tri-*n*-butylphosphine (carbon bonded to phosphorus, possessing one carbon and two hydrogen substituents), it would be better to model triisobutylphosphine, in which the carbon connected to the phosphorus has two carbon and one hydrogen substituent, with triisopropylphosphine.

If this argument seems familiar, it is because the results discussed thus far (geometric and charge-density derived) are consistent with that which would be expected based upon the Tolman electronic parameter ν [21]. In Fig. 5(A) and (B) are shown the plots of the Si–Pt bond distance, and the electron density at the bond critical point, against the experimental ν(phosphine) and the computed ν(silylene). In Fig. 5(A) it may be seen that while there is the aforementioned slight lengthening of the Si–Pt bond when the Y group is methyl while the phosphine substituent is hydrogen, the major change in the bond length occurs with the substitution of the phosphine hydrogen for methyl, indicating that the bond length, and therefore indirectly the strength of the Si–Pt bond, is influenced more by the choice of phosphine than by the silylene. Fig. 5(B) reinforces this view, with the density increasing by approximately 0.01 e/a_0^3. This graph nicely shows the interplay between the two ligands, since substituting only the silylene results in a decrease in density, due to a greater polarization of the electrons towards the silylene fragment. However, this effect is small, and somewhat exaggerated by the scale of the graph [22]. It does suggest, though, that the choice of phosphine is the most important in the design of these complexes, as it will determine the degree to which the metal center may engage in back-bonding with the silylene.

It it therefore demonstrated that that PMe_3, P^iPr_3, and PCy_3, while not identical, are similar in nature, while PH_3, which is commonly used a theoretical model for aliphatic phosphines, is more closely related to $P(OTolyl)_3$ or $P(OMe)_3$ [23]. For the purposes of modeling these complexes, therefore, we may extrapolate the results of the trihydrophosphine complex to postulated alkoxy or aryloxy phosphine metal silylenes, within the limitation that this is a purely electronic substitution, and does not, of course, account for steric differences. Furthermore, it means that when one is modeling these complexes, truncating the complex prematurely, such as using PH_3 to replace PCy_3, is a grave mistake, unless the groups that are being replaced are the aforementioned alkoxy or aryloxy. In order to

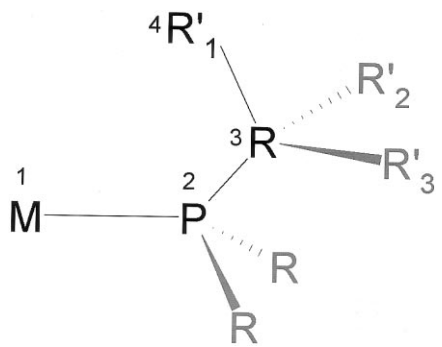

Fig. 4. Diagram of the 1-4 interaction, which determines the electron density, and hence the back-donation ability, of the platinum center.

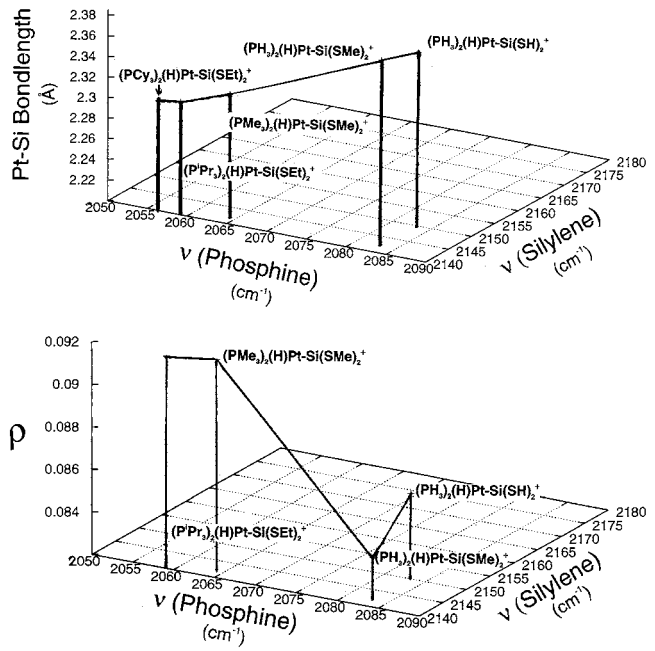

Fig. 5. (A) Plot of Pt–Si bond length against the Tolman electronic parameters for phosphine (experimental) and silylene (theoretical). Note that changing the substituent at silicon causes a minor perturbation of the bond distance, while changing the phosphine causes a marked shortening of the bond, until the cyclohexyl complex is reached. The change from phosphine to tricyclohexyl phosphine is worth approximately 0.1 Å, or roughly 5% of the bond distance, though most of this change has been recovered by the time H has been replaced by isopropyl. (B) Plot of the electron density at the Pt–Si bond critical point versus the Tolman parameters. Here it may be seen that substituting methyl for hydrogen at the silylene causes a slight distortion of the density, but that a much larger increase is seen when changing from phosphine to trimethyl phosphine. Once again, this indicates that the properties of the Pt–Si bond are determined primarily by the character of the substituents at phosphine, rather than by the characteristics of the silylene.

obtain a good description of an aliphatic phosphine, it may be necessary to explicitly include methyl, ethyl, or even isopropyl groups in order to have the requisite electron density available to the metal, through the aforementioned 1-4 interaction.

Further properties from the AIM analysis bear mentioning. The ellipticity of the charge density about the critical point of the Pt–Si bonds is curious, with the Pt–Si bond showing an average ellipticity (0.15) which is similar in magnitude to that of the Si–S bonds (0.16), which an earlier investigation indicated should possess significant π-character. The ellipticity is much greater than should be possessed by a system with only a single bond. In the latter, limiting case, the charge density about the Pt–Si bond should be cylindrical, and the resulting ellipticity near 0.0 [24]. Instead, with a value of greater than 0.1, it indicates significant deviation from the cylindrical ideal, and is strongly indicative of some degree of π-character. This measure of the degree of the Pt–Si π-bond is seemingly unperturbed by the character of the phosphines, remaining very close to 0.15 in all cases, although it decreases slightly when $R = PH_3$ and Y = Me, indicating the improved π-donor ability of the methylthiol group, and associated decrease of the Pt–Si π-bonding. It is therefore indicated that the bonding is more complicated than suspected previously, and that there are several resonance structures contributing to the overall bonding of the system which result in significant Si–M multiple bond character. The nature of the different bonding modes in the complex may be visualized more easily by viewing Fig. 6, the laplacian of the density of the complex $(PH_3)_2(H)PtSi(SH)_2^+$. Fig. 6(A) shows the plot of the laplacian of the electron density in the P–Pt–P plane, while Fig. 6(B) shows the density in the plane of the thiosilylene. In Fig. 6(A), it is apparent that there is a covalent interaction between the phosphorus and associated hydrogen, and an accumulation of electron density on the side of the phosphorus facing the metal, corresponding to a lone-pair being donated to the metal center. In a similar manner, there is a broad accumulation, similar to what would be expected of a bond containing π-character on the side of the silicon facing the metal. However, despite the accumulation of density at those points, the electron density remains concentrated in the spherical wells around the platinum and the silicon, which is consistent with a closed-shell

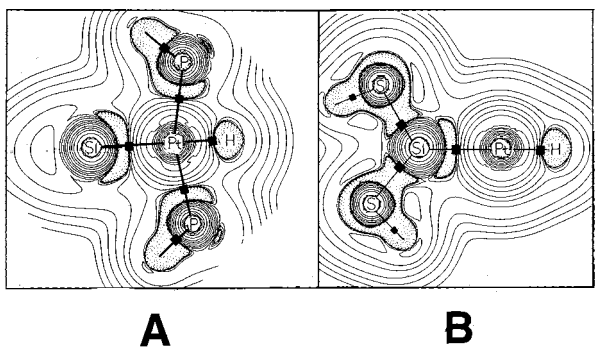

Fig. 6. (A) Plot of the laplacian of the electron density of $(PH_3)_2(H)Pt–Si(SH)_2^+$. Scale is 15 a.u. per side. (A) is in the Si–Pt–P plane, (B) is rotated 90° about the Pt–Si bond, and is in the plane of the thiosilylene. Dashed contours indicate an accumulation of electron density, while solid contours indicate a depletion. The boundry between the two defines the molecular reactive surface. Bond critical points are indicated as black squares. The accumulation of density in the Si–Pt–P plane versus the lesser accumulation in the perpendicular direction (B) nicely demonstrates the expected difference due to the presence of a π-bond. Note how (and in (B)) the system essentially splits into five components, all bound together through closed-shell interactions: the silylene fragment, two phosphines, the hydride, and the platinum. (B) Plot of the laplacian of the electron density in the plane of the thiosilylene (view is rotated 90° about the Pt–Si axis with respect to (A). Scale is 15 a.u. per side, dashed contours indicate an accumulation of electron density, while solid contours indicate a depletion. Despite the polarization of the electron density in the Si–S region, the interaction here remains closed-shell, or primarily ionic. Note the accumulation of density on the side of the silicon facing the platinum, but heavily polarized towards the silylene fragment.

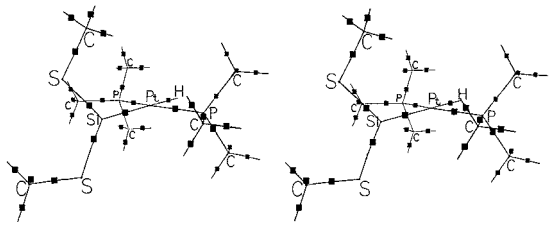

Fig. 7. Relaxed eye stereoplot of the bond paths (black lines) and bond critical points (black squares) in $(PMe_3)_2(H)PtSi(SMe)_2^+$. In the absence of steric congestion, the topology of the density remains simple and follows the anticipated paths based upon simple Lewis arguments, as opposed to the more complex topology shown in Fig. 8.

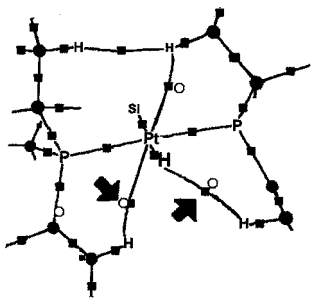

Fig. 8. Simplified view down the H–Pt–Si axis of some of the dihydrogen bonds, and their associated bond critical points (black squares) and ring critical points (white circles). Hydrogens are labeled to show how the path originates at a hydrogen, curves through the bond point to another nucleus, and has a closely associated ring critical point (indicated by the arrows in the diagram). A minor perturbation of the structure would cause some of these ring points to merge with their associated bond points, thereby annihilating each other, and breaking the bond. Extraneous atoms, critical points, and bonds removed for clarity.

interaction, such as our postulated donor–acceptor model. In passing we also note the broad region of density depletion parallel to the Si–Pt bond axis, which is in keeping with the strongly electrophilic nature of planar silylenes, and a visual demonstration of the reason for their tendency to bind Lewis bases. In Fig. 6(B) may be seen the silicon–sulfur bonding region, in which the density is somewhat more accumulated in the internuclear region than before, but still concentrated primarily in the atomic basins. The shape of the accumulation in the plane perpendicular to the Si–Pt–P plane is seen to be narrower in extent that the in-plane accumulation. This nicely shows the anticipated difference in the density between the perpendicular and parallel planes that one would expect from a π-bond. This picture is very similar to that shown by MacDougall and Hall [25] and Gillespie and coworkers [26] in their respective analyses of metal carbonyls and simple oxychlorides of the first row. For comparison, the sign and value of the laplacian of the S–C critical point in $(PMe_3)_2(H)PtSi(SMe)_2^+$ is -0.202 (e/a_0^5), versus 0.110 (e/a_0^5) for the Si–S, indicating the covalent nature of the C–S interaction and the closed-shell nature, and hence largely ionic, Si–S bond.

The character of the bonds is somewhat ambiguous, in that the two properties most commonly used to indicate the presence of a covalent, or closed-shell interaction, are somewhat at odds. In Table 2 it may be seen that the laplacian of the density is slightly positive for all of the systems, which indicates a weakly closed-shell interaction, while the energy density, $H(r)$, which is the sum of the kinetic and potential energies at the critical point [27], is slightly negative, indicating a bond that is weakly covalent. On the balance, this is probably indicative of the presence of several resonance forms of the bond existing, which leads to a mostly closed-shell description with some covalent character. This is similar to the picture derived in the earlier work on ruthenium silylenes [9], in which the value of the ruthenium to thiosilylene bond was a slightly higher -0.0434 (Hartree/a.u.^{3}). In contrast, Frenking and coworkers have reported energy densities in the range of -0.02 to -0.15 (Hartree/a.u.^{3}), in tungsten carbenes [28], and -0.03 to -0.07 (Hartree/a.u.^{3}) [29] in coinage metal silylenes and carbenes [30] which are approximately factor of two higher than those reported here in the case of the carbenes, and very similar for the silylenes. This demonstrates the less covalent nature of the platinum to thiosilylene bond versus the tungsten to carbene bond, and indicates that while evidence exists that the *N*-heterocyclic stabilized silylenes and carbenes react in a manner similar to the electron-rich phosphazines, in the end they are not significantly different from the demonstrably electron deficient thiosilylenes of this study [31].

The bond paths, which are the line of maximal density connecting the nuclear attractors with the bond critical points, are shown in Fig. 7 for $(PH_3)_2(H)Pt–Si(SH)_2^+$ and $(P^iPr_3)_2(H)Pt–Si(SEt)_2^+$ (Fig. 8, detail). While the former possesses a topology functionally identical to that predicted on the basis of traditional Lewis models, with straight bond paths connecting the nuclei with their associated bond critical points, the latter is more complex. We observe several features: first, there exist bond paths between hydrogens on the isopropyl groups and both the silicon and the sulfur centers. There is also a bond path between isopropyl hydrogens and the hydride ligand connected to the platinum, as well as some strongly curved bond paths between hydrogens on adjacted isopropyl groups within the phosphines. These features, while somewhat surprising, are independent of both basis set and integration parameters [32], and are therefore considered to be real properties of the electron density of the system, not artifacts of the analysis. They may be seen more clearly in Fig. 8, which is a view down the H–Pt–Si axis showing only the most important atoms, critical points, and bond paths.

Table 4
Hydrogen bond CPs for $(P^iPr_3)_2(H)Pt–Si(SEt)_2^+$ [a]

A	B	A–B			
		ρ	ε	$\nabla^2\rho$	*r*A–B
Si	H16	0.007	1.867	0.016	2.976
Si	H17	0.006	8.836	0.014	3.098
Pt	H33	0.011	0.982	0.032	2.895
Pt	H38	0.010	3.670	0.031	2.931
H(Pt)	H24	0.007	0.856	0.018	2.437
S	H45	0.003	0.254	0.014	3.265
H31	H19	0.006	0.620	0.018	2.415
H30	H19	0.010	0.090	0.031	2.061
H45	H33	0.003	0.254	0.011	3.265

[a] Units are: ρ (e/a_0^3), $\nabla^2\rho$ (e/a_0^5), $H(r)$ (Hartree/a_0^3).

Details of the bond critical points for these bonds paths are shown in Table 4. In all cases the density at the critical point is low, the laplacian is slightly positive, and the ellipticity is high, with the H–S bond and the close (2.061 Å) H30–H19 contact having ellipticities of 0.254 and 0.098, respectively. These latter two values are still high when compared with the expected value for a σ-type interaction, which would be zero. As may be seen in Fig. 8, all of these bond critical points have a closely associated ring critical point, which, along with the high ellipticities, indicates that the bond is unstable and subject to fission with only minor structural distortions. This is consistent with these points representing hydrogen–hydrogen bonds which stabilize the structure in the minimal conformation, but which would be easily disrupted by molecular vibrations and solvent–solute interactions under normal, synthetic conditions.

In the case of the Si···H, S···H, and hydride···H interactions, these may be explained as arising from charge separations between the hydrogen and adjacted atoms. Crabtree and coworkers have noted from a study of structures in the Cambridge Crystallographic Database that many metal complexes possess hydrogen–hydrogen Hydrogen bonds (called dihydrogen bonds by Crabtree, et al.), of the general form D–H···H–A, where D is an electron rich center, and A is an electron deficient [33]. Popelier has further shown that this is a general property of systems possessing charge separation, with his AIM study of H_3BNH_3 dimers [34]. Given the strongly electron deficient nature of the silicon, the electron rich nature of the sulfurs, the charge differences between the hydride coordinated to metal versus the isopropyl protons on the ligands, and the sterically congested structure, it should not be considered surprising that these features are found to arise in this system. It is important to note that these interactions are not seen in the less sterically crowded complexes with trimethylphosphine, or phosphine as ligands, and so they may be considered to be 'interactions of opportunity', which contribute to overall stabilization of the structure, but are not vital to its existence. In the real world, these are features that would probably be observed primarily under low-density gas phase conditions, or in the solid state, where molecular motion is strongly hindered, rather than in solution where solvent interactions would tend to disrupt these bonds. It is also important to realize that the definition of a bond within the AIM framework is an expression of the curvature of the electron density between two centers, and does not necessarily imply any certain number of electrons being shared. Most of these non-traditional bonds that we are discussing here are strongly curved, which has been observed previously within the context of electron deficient bonding, such as in boranes [35]. The properties of these bonds are shown in Table 4, where it is observed that while the values of the electron density at the critical points is lower than seen in the other bonds, it is consistent with previously reported values for hydrogen bonds, and should therefore be considered to arise from real, albeit weak, interactions [36].

Table 5 shows the CDA results for the fragments $Si(SY)_2$ and $(H)Pt(PR_3)_2^+$. CDA presumes the molecule to be describable in terms of the Dewar–Chatt–Duncanson 'donor–acceptor' model [37], that is, interactions between closed-shell fragments. Surprisingly, a high degree of back-donation from metal to thiosilylene is seen in all cases, which indicates that despite the strong S–Si interaction, there also exists a Si–M π interaction. The degree of donation and back-donation increases from 0.52d (0.23a) to 0.54d (0.39a), with the back-donation increasing more rapidly, leading to a decrease in the d/a ratio, from 2.4 to approximately

Table 5
CDA of $Y_2Si\cdots Pt(H)(PR_3)_2^+$

R	Y	Donate	Back	d/a	Binding [a] (kcal/mol)	Residual	Repulsion
H	H	0.517	0.215	2.40	50.92	0.015	−0.227
H	Me	0.550	0.205	2.68	56.70	0.007	−0.208
Me	Me	0.525	0.268	1.96	51.74	0.015	−0.300
^{i}Pr	Et	0.549	0.354	1.55	50.20	0.010	−0.409
Cy	Et	0.541	0.351	1.53	49.89	0.007	−0.413

[a] Binding energy in the context of CDA is energy of the total system − the energy of the fragments. See text for elaboration.

Table 6
CDA analysis of $(PR_3)_2\cdots(H)PtSi(SY)_2^+$

R	Y	Donate	Back	d/a	Binding (kcal/mol)	Residual	Repulsion
H	H	0.381	0.132	2.89	72.05	0.004	−0.213
H	Me	0.370	0.136	2.72	69.89	0.010	−0.219
Me	Me	0.234	0.089	2.63	99.84	0.040	0.027
^{i}Pr	Et	0.333	0.099	3.36	100.45	0.015	−0.138
Cy	Et	0.374	0.113	3.31	100.07	−0.027	−0.227

1.55. This results in a bond that is less polarized in the more substituted systems (R = ^{i}Pr, Cy) than in the more open ones (R = H, Me). It also creates a charge redistribution which creates a slight positive charge on the silylene fragment, which decreases as the donating ability of the phosphorus ligand set increases.

Despite the increased interaction between the fragments, and the decrease in the bond-polarization, The *E*(snap) values remain constant. This arises from the increased repulsion term, which indicates that while the interaction between the Si and Pt fragments grows stronger, the greater bulk of the ligands increases the steric interactions, and serve to destabilize the molecule by a similar amount. Thermodynamically, therefore, there is no advantage in using a phosphine larger than methyl, since it results in destabilization of the bond due to steric congestion, though it does allow tuning of the strength of the π-character, which may be important synthetically.

The trends in the binding by phosphine from CDA analysis are shown in Table 6. As would be expected, the aliphatic phosphines all have poor π-acceptor natures, as shown by the high donation to acceptance (d/a) ratios of 2.64 to 3.36. As was seen in the case of the earlier fragment analysis, the system has essentially stabilized from an electronic point of view by the time that R = isopropyl. There exists a discontinuity in the d/a trend when the substituent on phosphorus is methyl, since the unsubstituted methyl groups are sufficiently electronegative to compete successfully with the platinum–silylene unit for electron density. When two of the methyl protons are replaced with further methyl groups, the charge at the phosphorus decreases, which improves its ability to act as an electron donor, leading the number of electrons donated to converge to approximately 0.33. These trends should be viewed as primarily qualitative, since the parent diphosphine fragment is capable of P–P interactions which perturb the final results, but provide a useful guide for choosing a particular model phosphine over other candidates.

It has recently been suggested that the bonding in heavy main-group to metal complexes would be better classified in terms of donor–acceptor character and ionic nature, rather than in the language of single, double, and triple bonds.[38] While this position has merit, the balanced donor–acceptor character of these model systems, with d/a ratios near 1.0, and the single π-type orbital available on silicon, leads to the conclusion that it is still appropriate to speak of 'double bond character' in the case of these complexes. It is, however, a matter that should be taken under consideration in other, less clear-cut, situations.

4. Conclusion

Cationic, 4-coordinate, platinum thiosilylenes possess significant Pt–Si multiple bond character, as well as Si–S multiple bond character. The system may be thought of as possessing several, nearly balanced, resonance structures, in which Si–S π-interactions are sufficient to protect the silicon against attack by solvent Lewis bases, and decrease the acceptor ability of the Si fragment. It should therefore be possible to exploit the Pt=Si double bond using conventional synthetic techniques. The four-coordinate design, while successful for carbenes, is less so for silicon due to the strong susceptibility of the electropositive silylene fragment to the *trans* effect. Further investigations in this area are in progress.

References

[1] See, for instance: (a) T.D. Tilley, in: The Silicon–Heteroatom Bond, S. Patai, Z. Rappaport (eds.), New York: Wiley, 1991, pp. 245 and 290 (Chapters 9 and 10). (b) J. Corey, in: Advances in Silicon Chemistry, vol. 1, G. Larson (ed.), Greenwich, CT: JAI Press, 1991, p. 327. (c) C. Zybill, Top. Curr. Chem. 160 (1990) 1. (d) K.H. Pannell, H.K. Shama, Chem. Rev. 95 (1995) 1351. (e) T.R. Cundari, M.S. Gordon, Organometallics 11 (1992) 3122. (f) T.R. Cundari, M.S. Gordon, J. Phys. Chem. 96 (1992) 631. (g) H. Jacobsen, T. Ziegler, Inorg. Chem. 35 (1996) 775.
[2] W. Kutzelnigg, Angew. Chem. Int. Ed. Engl. 23 (1984) 272.
[3] C. Zybill, H. Handwerker, H. Friedrich, in: Advances in Organometallic Chemistry, vol. 36, New York: Academic, 1994, p. 229 and references cited therein.
[4] For example, see: (a) R.J.P. Corriu, B.P.S. Chauhan, G.F. Lanneau, Organometallics 14 (1995) 4014. (b) R.J.P. Corriu, B.P.S. Chauhan, G.F. Lanneau, Organometallics 14 (1995) 1646. (c) B.P.S. Chauhan, R.J.P. Corriu, G.F. Lanneau, C. Priou, N. Auner, H. Handwerker, E. Herdtweck, Organometallics 14 (1995) 1657.

[5] (a) D.A. Straus, S.D. Grumbine, T.D. Tilley, J. Am. Chem. Soc. 112 (1990) 7801. (b) S.D. Grumbine, T.D. Tilley, A.L. Rheingold, J. Am. Chem. Soc. 115 (1993) 358. (c) S.D. Grumbine, T.D. Tilley, F.P. Arnold, A.L. Rheingold, J. Am. Chem. Soc. 115 (1993) 7884. (d) H. Handwerker, M. Paul, J. Blumel, C. Zybill, Angew. Chem. 105 (1993) 1375; Angew. Chem. Int. Ed. Engl. 32 (1993) 1313. (e) C.E. Zybill, C.Y. Liu, Synlett 7 (1995) 687. (f) C. Leis, C. Zybill, J. Lachmann, G. Müller, Polyhedron 10 (1991) 1163. (g) M. Denk, R.K. Hayashi, R. West, J. Chem. Soc. Chem. Commun. (1994) 33. (h) S.K. Grumbine, G.P. Mitchell, A. Straus, T.D. Tilley, Organometallics 17 (1998) 5607.
[6] H. Jacobsen, T. Ziegler, Organometallics 14 (1995) 224.
[7] M.B. Hall, R.F. Fenske, Inorg. Chem. 11 (1972) 768.
[8] S.K. Grumbine, T.D. Tilley, F.P. Arnold, A.L. Rheingold, J. Am. Chem. Soc. 116 (1994) 5495.
[9] F.P. Arnold, Organometallics 19 (1999) 4800.
[10] Gaussian 98 (Revision A.7), M.J. Frisch, G.W. Trucks, H.B. Schlegel, G.E. Scuseria, M.A. Robb, J.R. Cheeseman, V.G. Zakrzewski, J.A. Montgomery, R.E. Stratmann, J.C. Burant, S. Dapprich, J.M. Millam, A.D. Daniels, K.N. Kudin, M.C. Strain, O. Farkas, J. Tomasi, V. Barone, M. Cossi, R. Cammi, B. Mennucci, C. Pomelli, C. Adamo, S. Clifford, J. Ochterski, G.A. Petersson, P.Y. Ayala, Q. Cui, K. Morokuma, D.K. Malick, A.D. Rabuck, K. Raghavachari, J.B. Foresman, J. Cioslowski, J.V. Ortiz, B.B. Stefanov, G. Liu, A. Liashenko, P. Piskorz, I. Komaromi, R. Gomperts, R.L. Martin, D.J. Fox, T. Keith, M.A. Al-Laham, C.Y. Peng, A. Nanayakkara, C. Gonzalez, M. Challacombe, P.M.W. Gill, B.G. Johnson, W. Chen, M.W. Wong, J.L. Andres, M. Head-Gordon, E.S. Replogle, J.A. Pople, Gaussian, Inc., Pittsburgh, PA, 1998.
[11] Addition of d-functions to the carbons during the optimization did not appreciably chance the geometry of the complexes $(Cy_3P)_2(H)Pt–Si(SEt)_2^+$ and $(Me_3P)_2(H)Pt–Si(SH)_2^+$. Since the carbon atoms are not directly attached to the framework Pt or Si, and their valences are saturated and sp^3 hybridized, this ommission is not expected to cause difficulties. F.P. Arnold, D.M. Potts, unpublished results.
[12] S. Dapprich, G. Frenking, J. Phys. Chem. 99 (1995) 9352.
[13] CDA requires closed-shell fragments. This choice of fragments results in a neutral silylene fragment with two electrons available for σ-donation, and a vacant π-orbital capable of accepting two electrons, as well as a cationic metal center.
[14] It is recognized that in light of Ref. [12], this basis set is slightly smaller than that recommended by Frenking et al., but was chosen so as to allow a consistent basis set to be applied to all four systems, given the size of the experimentally characterized complex, $(Cy_3P)_2(H)Pt–Si(SEt)_2^+$.
[15] Huzinaga, S. (ed.) et al., Gaussian Basis Sets for Molecular Calculations, 1984, Amsterdam: Elsevier, The Netherlands, p. 362.
[16] Ibid, $\zeta(p) = (0.102, 0.033)$
[17] R.F.W. Bader, Atoms In Molecules, a Quantum Theory, Oxford University Press, Oxford, UK, 1994.
[18] F. Biegler-König, J. Schönbohm, R. Derdau, D. Bayles, R.F.W. Bader, AIM2000 version 1.0, http://gauss.fh-bielefeld.de/aim2000/index.htm
[19] For a brief overview of relativistic effects, and applications specific to platinum, see: (a) P. Pyykkö, Chem. Rev. 88 (1988) 563. (b) J. Li, G. Schreckenbach, T. Ziegler, Inorg. Chem. 34 (1995) 3245. (c) M. Pepper, B.E. Bursten, Chem. Rev. 91 (1991) 719. (d) T.M. Gilbert, T. Ziegler, J. Phys. Chem. A 103 (1999) 7535. (e) R. Stranger, G.A. Medley, J.E. McGrady, J.M. Garrett, T.G. Appleton, Inorg. Chem. 35 (1996) 2268.
[20] It has been pointed out by one reviewer that in the case of octahedral carbenes and silylenes, there exists no rotational barrier due to effectively cylindrical symmetry of the d_{xz}/d_{yz} orbitals, which is correct. However, in the case of square planar 16 electron complexes, there exists a rotational barrier. Examples, calculated at the same level of theory as this paper: $(PMe_3)_2(H)PtSiMe_2^+$ possesses a rotational barrier of almost 9 kcal/mol (uncorrected for zero-point energy and entropy). Strengthening of the Pt–Si π-bond, or increasing the steric bulk, would increase this value.
[21] C.A. Tolman, Chem. Rev. 77 (1977) 313, Appendix A.
[22] The densities at the bond midpoint in ethylene and silylethylene ($H_2C{=}SiH_2$) are 0.344 and 0.147, with values of $\nabla^2\rho$ at the critical point of -1.03 and 0.527, indicating the first to be a covalent bond, while the second possesses a large degree of closed-shell, donor–acceptor character. Arnold, F.P., unpublished results.
[23] The author regrets that computer time/space constraints precluded including results from calculations involving alkoxy ligands on phosphorus. That subject will be dealt with in a subsequent paper, currently in preparation. F.P. Arnold, D.M. Potts, in preparation.
[24] For comparison, the ellipticity of the heavy-atom bond in the case of ethylene and silylethylene ($H_2C{=}SiH_2$) is 0.332 and 0.486, respectively, with the latter value reflecting the non-planar nature of the Si–C bond. F.P. Arnold, unpublished results.
[25] P.J. MacDougall, M.B. Hall, Transact. Am. Cryst. Assoc. 26 (1990) 105.
[26] R.J. Gillespie, I. Bytheway, T.-H. Tang, R.F.W. Bader, Inorg Chem. 35 (1996) 3954.
[27] D. Cremer, E. Kraka, Angew. Chem. Int. Ed. Engl. 23 (1984) 627.
[28] (a) U. Pidun, G. Frenking, Organometallics 14 (1995) 5325. (b) G. Frenking, U. Pidun, J. Chem. Soc. Dalton Trans. (1997) 1653.
[29] Presuming a conversion of 1 a.u.^{3} = 0.14818462 Å^3.
[30] C. Boehme, G. Frenking, Organometallics 17 (1998) 5801.
[31] W.A. Herrman, C. Köcher, Angew. Chem. Int. Ed. Engl. 36 (1997) 2162.
[32] Because of the complex topology, various adjustment to the integration parameters were made, as well as comparing with the density from a calculation with the 6-311 + + G** basis set on the main-group atoms, and the LANL2DZ ECP + DZ valence basis set, and with the 6-311 + G* basis set for the main group atoms, and the aforementioned ECP + valence basis set. The latter, due to the lack of f-functions in the wavefunction, were analyzed with both Bader's AIM package, and with Popelier's MORPHY 1.0, which uses an eigenvector following algorithm rather than a Newton-Raphson in order to find the critical points. In all cases the bond paths and critical points remained the same.
[33] T.B. Richardson, S. de Gala, R.H. Crabtree, P.E.M. Siegbahn, J. Am. Chem. Soc. 117 (1995) 12875.
[34] P.L.A. Popelier, J. Phys. Chem. A. 102 (1998) 1873.
[35] R.F.W. Bader, D.A. Legare, Can. J. Chem. 70 (1992) 657.
[36] U. Koch, P. Popelier, J. Phys. Chem. 99 (1995) 9747.
[37] (a) M.J.S. Dewar, Bull. Chem. Soc. Fr. 18 (1951) C79. (b) J. Chatt, L.A. Duncanson, J. Chem. Soc. (1953) 2929.
[38] C. Boehme, G. Frenking, Chem. Eur. J. 5 (1999) 2184.